

Laser action in chromium-doped forsterite

V. Petričević, S. K. Gayen, and R. R. Alfano

Institute for Ultrafast Spectroscopy and Lasers, Photonics Application Laboratory, Departments of Physics and Electrical Engineering, The City College of New York, New York, New York 10031

Kiyoshi Yamagishi, H. Anzai, and Y. Yamaguchi

Electronic Materials Research Laboratory, Mitsui Mining and Smelting Co., Ltd., 1333-2 Haraichi, Ageo-Shi, Saitama 362, Japan

(Received 7 December 1987; accepted for publication 1 February 1988)

Room-temperature vibronic pulsed laser action in trivalent chromium-activated forsterite ($\text{Cr}^{3+}:\text{Mg}_2\text{SiO}_4$) is reported for the first time. The free-running laser emission is centered at 1235 nm of the broad ${}^4T_2 \rightarrow {}^4A_2$ fluorescence band, and has a bandwidth of ~ 22 nm.

Prompted by the successful broadly wavelength-tunable, room-temperature operation of alexandrite¹ and emerald^{2,3} lasers, the surge in research activities on tunable solid-state lasers has been extensive in the 1980s.⁴⁻¹⁷ The thrust of these research endeavors has been twofold: first to look for new host materials for the trivalent chromium ion,⁷⁻¹¹ and second, to search for new ions that will lase in commonly used host crystals.^{4-6,12-17} These efforts have been rewarded by the successful wavelength-tunable laser operation of Cr^{3+} in a number of hosts,⁷⁻¹¹ by the discovery of new lasing ions trivalent titanium (Ti^{3+})^{6,12,13} and divalent rhodium¹⁶ (Rh^{2+}), as well as by the "rediscovery"^{4,5,14,15,17} of tunable phonon-terminated lasers based on divalent transition metal ions Ni^{2+} , Co^{2+} , and V^{2+} . In this letter, we present the first room-temperature vibronic pulsed laser operation of Cr^{3+} in forsterite (Mg_2SiO_4).

Forsterite, like alexandrite, is a member of the olivine family of crystals. It is a naturally occurring gem. Single crystals of forsterite may be grown by the Czochralski method. A unit cell of forsterite has four formula units in an orthorhombic structure of the space group $Pbnm$.¹⁸ The unit cell dimensions are: $a = 4.76$ Å, $b = 10.22$ Å, and $c = 5.99$ Å. The Cr^{3+} ion substitutes for the Mg^{2+} ion in two distinct octahedrally coordinated sites: one (M1) with inversion symmetry (C_i), and the other (M2) with mirror symmetry (C_s). The occupation ratio of the two sites¹⁹ by the Cr^{3+} ion is M1:M2 = 3:2.

The single crystal of $\text{Cr}^{3+}:\text{Mg}_2\text{SiO}_4$ used for spectroscopic and laser action measurements was grown by the Czochralski method at the Electronic Materials Research Laboratory of the Mitsui Mining and Smelting Co., Ltd., Japan. The crystal is a 9 mm \times 9 mm \times 4.5 mm rectangular parallelepiped with the three mutually orthogonal axes oriented along the b , c , and a crystallographic axes of the crystal. The crystal contains 0.04 at. % of Cr^{3+} ions, which is equivalent to a chromium ion concentration of 6.9×10^{18} ions/cm³.

The room-temperature fluorescence and absorption spectra of $\text{Cr}^{3+}:\text{Mg}_2\text{SiO}_4$ for $E \parallel b$ crystallographic axis are shown in Fig. 1. The fluorescence spectrum of $\text{Cr}^{3+}:\text{Mg}_2\text{SiO}_4$ was excited by the 488-nm radiation from an argon-ion laser and recorded by a germanium photodiode detector lock-in amplifier combination at the end of a 0.25-m monochromator equipped with a 1000-nm blazed grating. The

room-temperature spectrum is a broad band covering the wavelength range 700–1400 nm. The room-temperature fluorescence lifetime is 15 μs .

The absorption spectrum was taken with a Perkin-Elmer Lambda-9 spectrophotometer along the 4.5-mm path length of the sample. It is characterized by two broad bands centered at 740 and 460 nm attributed to the ${}^4A_2 \rightarrow {}^4T_2$ and ${}^4A_2 \rightarrow {}^4T_1$ absorptive transitions, respectively, of the Cr^{3+} ion. The broad, weak absorption band between 850 and 1150 nm is not observed in the excitation spectrum.²⁰ This indicates that the origin of this absorption is not transitions in Cr^{3+} ion, but in some other impurity ions, e.g., Fe^{3+} in the host crystal.²¹ It is evident from Fig. 1 that this background absorption overlaps a significant spectral region of $\text{Cr}^{3+}:\text{Mg}_2\text{SiO}_4$ emission, and inhibits laser action in that region.

The experimental arrangement for investigating the laser action²² in $\text{Cr}^{3+}:\text{Mg}_2\text{SiO}_4$ is shown schematically in Fig. 2. The sample is placed at the center of a stable resonator formed by two 30-cm-rad mirrors placed 20 cm apart. The mirrors were dielectric coated to transmit the 532-nm pump beam, and to have high reflectivity in the 1150–1250 nm spectral range. The reflectivity of the back mirror M_1 is 99.9%, while that of the output mirror M_2 is $\sim 98\%$ for normal incidence over the specified wavelength range. It is

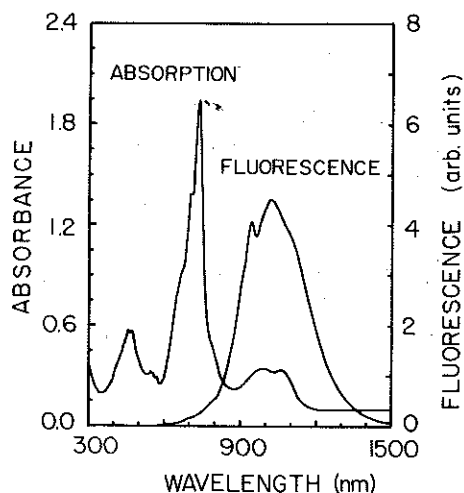


FIG. 1. Absorption and fluorescence spectra of $\text{Cr}^{3+}:\text{Mg}_2\text{SiO}_4$ at room temperature. Both the spectra were taken for $E \parallel b$ axis and excitation along a axis. The thickness of the sample along a axis is 4.5 mm.

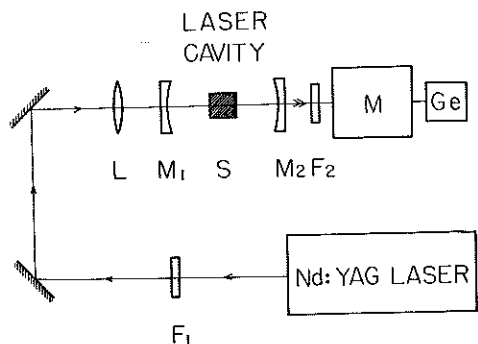


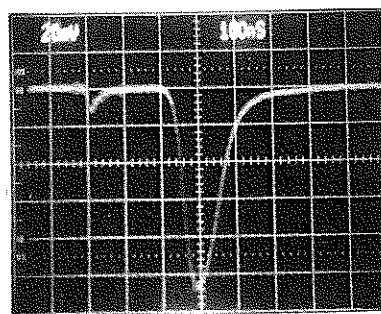
FIG. 2. Schematic diagram of the experimental arrangement for investigating laser action in $\text{Cr}^{3+}:\text{Mg}_2\text{SiO}_4$. (Key: $F_1 = 1060\text{-nm}$ blocking filter, $F_2 = 532\text{-nm}$ blocking infrared transmitting filter, $M_1 = \text{back mirror}$, $M_2 = \text{output mirror}$, $L = \text{lens}$, $S = \text{sample}$, $\text{Ge} = \text{germanium photodiode detector}$, $M = \text{monochromator}$.)

to be noted that this spectral region does not correspond to the peak of the fluorescence spectrum, but was chosen so that the background absorption is minimal. The sample was longitudinally pumped by frequency-doubled 532-nm, 10-ns full width at half maximum (FWHM) pulses from a Q-switched Nd:YAG laser (Quanta Ray DCR-1) operating at a 10-Hz repetition rate. The spatial profile of the pump pulse was a doughnut, characteristic of an unstable cavity. The pump beam was linearly polarized along the b axis and propagated along the a axis of the sample. It was focused 3 cm before the sample by a 25-cm focal length lens. The radius of the pump beam at the center of the sample is $\sim 600\ \mu\text{m}$. The output from the laser cavity was analyzed by a 0.25-m monochromator and monitored by a germanium photodiode detector. The output of the detector was displayed on a fast oscilloscope. No dispersive element was placed in the cavity and the laser operated in a free-running pulsed mode.

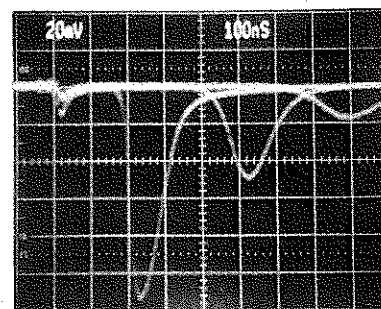
Pulsed laser operation was readily obtained for pumping at or above the lasing threshold of 2.2 mJ. A single output laser pulse was obtained, implying a gain-switched operation which is a consequence of pump-pulse duration being shorter than the lasing-level lifetime. The amplitude and duration of the laser pulse varied, as expected, with the pulse-to-pulse energy fluctuation of the pump laser. The output was extremely sensitive even to a small misalignment of the cavity, or insertion of a glass plate (8% loss) in the cavity.

The temporal profile of the $\text{Cr}^{3+}:\text{Mg}_2\text{SiO}_4$ laser pulse is shown in Fig. 3(a), and fluctuations in its amplitude, duration, and delay with respect to the pump pulse are displayed in Fig. 3(b). The temporal duration (FWHM) of the output laser pulse varied from 200 ns at the threshold to 100 ns at 2.4 times the threshold energy. The delay between the peak of the pump pulse and the peak of the $\text{Cr}^{3+}:\text{Mg}_2\text{SiO}_4$ laser pulse also varied, as expected, with pump-pulse energy, from 700 ns at the threshold to 200 ns at 2.4 times the threshold energy. This indicates that the laser cavity is highly lossy, and several hundred round trips are required to build up the laser oscillation in the cavity.

The laser threshold and slope efficiency were measured for the cavity used in this experiment and the data are displayed in Fig. 4. The laser oscillation starts to build up at an absorbed input energy of 2.2 mJ. The measured slope effi-



(a)



(b)

FIG. 3. Temporal profile and delay with respect to the pump pulse of the $\text{Cr}^{3+}:\text{Mg}_2\text{SiO}_4$ laser pulse: (a) a single pulse for pump energy 1.7 times the threshold energy; and (b) three pulses for pump energies near (right), twice (middle), and 2.4 times (left) the threshold energy. The narrow pulse at the extreme left of both the oscilloscope traces is the leakage of the pump pulse. For this measurement the monochromator was removed and filters were adjusted to allow a small leakage of pump pulse. The time and voltage scales are 100 ns/div and 20 mV/div, respectively.

ciency of 1.4% is rather low, and indicates large losses in the cavity. These losses include $\sim 13\%$ reflection loss from the uncoated sample surfaces, scattering from inhomogeneities in the crystal, and a large mismatch between the size of the pump beam and the $\text{Cr}^{3+}:\text{Mg}_2\text{SiO}_4$ cavity modes in the sample.

The spectrum of $\text{Cr}^{3+}:\text{Mg}_2\text{SiO}_4$ laser is shown in Fig. 5, for an absorbed pump energy of 3.4 mJ. The spectrum peaks at 1235 nm and has a bandwidth (FWHM) of 22 nm. The wide spectrum of the laser output can be used to pro-

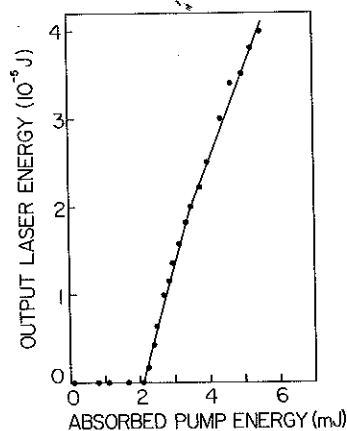


FIG. 4. Output energy of $\text{Cr}^{3+}:\text{Mg}_2\text{SiO}_4$ laser as a function of input energy.

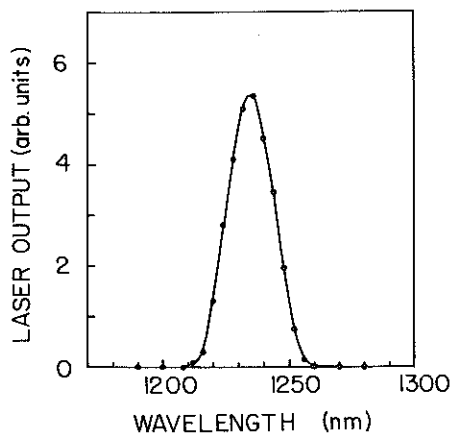


FIG. 5. Spectrum of free-running $\text{Cr}^{3+}:\text{Mg}_2\text{SiO}_4$ laser.

duce femtosecond pulses. The spectral range is limited at the high-energy end by the mirror transmission and the impurity absorption, while at the low-energy end by the mirror transmission as well as by the decrease in fluorescence intensity. Using different sets of mirrors, laser action in the 1.1–1.3 μm spectral range can be obtained.

In summary, pulsed laser operation has been obtained in $\text{Cr}^{3+}:\text{Mg}_2\text{SiO}_4$ at room temperature. The laser emission is centered at 1235 nm and has a bandwidth of ~ 22 nm. The spectral range for laser emission is expected to extend from 850 to 1300 nm if the parasitic impurity absorption may be minimized by improved crystal growth technique, making it one of the most widely tunable solid-state lasers in this spectral region. The large fluorescence bandwidth of the crystal promises ultrashort pulse generation through mode-locked operation. The fluorescence lifetime of 15 μs is suitable for effective energy storage and high-power Q -switched operation.

We would like to acknowledge Professor Roger Dorsinville for helpful discussions and Teruo Hiruma for help and support. The research is supported by National Aeronautics and Space Administration, Army Research Office, Hamamatsu Photonics, and City College of New York Organized Research.

- ¹J. C. Walling, O. G. Peterson, H. P. Jenssen, R. C. Morris, and E. Wayne O'Dell, *IEEE J. Quantum Electron.* **QE-16**, 1302 (1980) and references therein.
- ²M. L. Shand and J. C. Walling, *IEEE J. Quantum Electron.* **QE-18**, 1829 (1982).
- ³J. Buchert, A. Katz, and R. R. Alfano, *IEEE J. Quantum Electron.* **QE-19**, 1477 (1983).
- ⁴P. F. Moulton, *IEEE J. Quantum Electron.* **QE-21**, 1582 (1985).
- ⁵P. F. Moulton, *IEEE J. Quantum Electron.* **QE-18**, 1185 (1982).
- ⁶P. F. Moulton, *J. Opt. Soc. Am. B* **3**, 125 (1986) and references therein.
- ⁷B. Struve, G. Huber, V. V. Laptev, J. A. Scherbakov, and Y. V. Zharikov, *Appl. Phys. B* **28**, 235 (1982).
- ⁸U. Brauch and U. Dürr, *Opt. Commun.* **49**, 61 (1984).
- ⁹H. P. Jenssen and S. T. Lai, *J. Opt. Soc. Am.* **3**, 115 (1986).
- ¹⁰W. Kolbe, K. Petermann, and G. Huber, *IEEE J. Quantum Electron.* **QE-21**, 1596 (1985).
- ¹¹S. T. Lai, B. H. T. Chai, M. Long, and R. C. Morris, *IEEE J. Quantum Electron.* **QE-22**, 1931 (1986).
- ¹²G. M. Loiacono, M. F. Shone, G. Mizell, R. C. Powell, G. J. Quarles, and B. Elouadi, *Appl. Phys. Lett.* **48**, 622 (1986).
- ¹³A. I. Alimpiev, G. V. Bukin, V. N. Matrosov, E. V. Pestryakov, V. P. Solntsev, V. I. Trunov, E. G. Tsvetkov, and V. P. Chebotaev, *Sov. J. Quantum Electron.* **16**, 579 (1986).
- ¹⁴U. Brauch and U. Dürr, *Opt. Commun.* **55**, 35 (1985).
- ¹⁵W. Knierim, A. Honold, U. Brauch, and U. Dürr, *J. Opt. Soc. Am. B* **3**, 119 (1986) and references therein.
- ¹⁶R. C. Powell, G. J. Quarles, J. J. Martin, C. A. Hunt, and W. A. Sibley, *Opt. Lett.* **10**, 212 (1985).
- ¹⁷P. F. Moulton and A. Mooradian, *Appl. Phys. Lett.* **35**, 838 (1979).
- ¹⁸J. R. Smyth and R. M. Hazen, *Am. Mineral.* **58**, 588 (1973).
- ¹⁹L. V. Bershov, J. M. Gaite, S. S. Hafner, and H. Rager, *Phys. Chem. Minerals* **9**, 95 (1983).
- ²⁰K. Yamagishi (unpublished).
- ²¹W. A. Runciman, D. Sengupta, and J. T. Gourley, *Am. Mineral.* **58**, 451 (1973).
- ²²R. R. Alfano, V. Petričević, and S. K. Gayen, U.S. Patent pending.